

# A Design Methodology for Robust Model-Based Fault Diagnosis Schemes and its Application to an Aircraft Hydraulic Power Package

Felix Mardt<sup>1</sup>, Phillip Bischof<sup>2</sup> and Frank Thielecke<sup>3</sup>

<sup>1,2,3</sup> Institute of Aircraft Systems Engineering – Hamburg University of Technology, Hamburg, 21129, Germany

*felix.mardt@tuhh.de*

*phillip.bischof@tuhh.de*

*frank.thielecke@tuhh.de*

## ABSTRACT

In a system's design phase, where knowledge about the actual behavior of the system is shallow, the design of an efficient and robust system diagnostics is a complex task. In order to simplify this process, this paper presents a model-based methodology for the design of fault diagnosis schemes. The methodology analyzes the structure of available behavioral models of the system and proposes minimal sets of sensors to fulfill diagnostic requirements. In order to choose an optimal set of sensors, the method evaluates the sets in terms of costs and diagnostic robustness. The proposed fault detection, isolation and identification schemes rely on the robust evaluation of model-based residuals using Monte-Carlo methods and highest density regions to account for measurement and parameter uncertainty. To show the design capabilities, the presented method is applied to an aircraft hydraulic power package and the resulting schemes are tested on a real test rig.

## 1. INTRODUCTION

The highly competitive nature of the aviation industry requires the optimization of every aspect of an aircraft's life cycle. Thus, the optimization of aircraft maintenance being one of the biggest contributors to the direct operating costs is a prominent research field. Several new concepts such as condition-based, predictive or prescriptive maintenance have been developed which aim at a condition or health oriented maintenance in contrast to the historical preventive maintenance strategies. The key enabler for all of these new strategies is on-board fault diagnosis. Fault diagnosis is the umbrella term for the full sensor-based health assessment and consists of fault detection, isolation and, if applicable, identification (FDII). The design of an efficient and robust fault diagnosis scheme, which includes the selection of sensors as

well as the algorithms for the different layers, is a difficult task. Especially during the design phase of complex systems where the knowledge about the actual behavior of the system is shallow, it is not trivial to find a set of sensors which fulfills the robustness and FDII requirements in an optimal manner.

To support this task, this paper presents a methodology for the design of a robust model-based fault diagnosis scheme which supports the designer by utilizing knowledge contained in behavioral models of the system. These models are generally available in modern model-based engineering processes and can be exploited for diagnosis design during a system's design phase. This shortens the overall development by saving design iteration and testing time.

This paper is structured as follows. Section 2 describes the chosen concept of how models are used to diagnose a system, as well as the implementation of these concepts to a system as an FDII engine. The methodology to derive an FDII engine from a behavioral model of the system is presented in Section 3. To assess the applicability, the concept is applied to a hydraulic power package in Section 4. The paper closes with conclusions and remarks in Section 5.

## 2. MODEL-BASED FAULT DIAGNOSIS

As mentioned in the introduction, behavioral models are a sound source of knowledge during a system's design phase, which originates from the physical base most behavioral models are built on. These physical relations are therefore explainable and comprehensible. This comes with the downside of generally complex, non-linear and dynamic equations, which require costly calculations to solve. Therefore, a lot of FDII methods rely on linear models, which are generally less computationally expensive and allow the use of the well understood theory of linear systems. Since linear models are usually only applicable in a limited space of operation and the scope of the methods discussed in this paper is maintenance FDII which is usually not as time critical as its safety related counterpart, the full non-linear equations shall be used.

Felix Mardt et al. This is an open-access article distributed under the terms of the Creative Commons Attribution 3.0 United States License, which permits unrestricted use, distribution, and reproduction in any medium, provided the original author and source are credited.

Another downside of using these non-linear dynamic models is that their solution depends on initial values and convergence. Thus, making it not only computationally expensive but limiting their robustness. It is assumed that most of the maintenance-relevant faults can be detected using steady-state relations which ignore the dynamics and remove the complexity of solving dynamic models. Thus, the chosen method shall use full non-linear steady-state models. The following section describes the utilization of non-linear steady-state equations for FDII in general and how the general method is applied to an actual system.

## 2.1. Utilizing Non-Linear Models for Fault Detection Isolation and Identification

Consider a model  $M$  of some physical process  $P$

$$P \sim M = \{e, x, y, \theta, f\}, \quad (1)$$

where  $M$  consists of equations  $e$  with unknown internal states  $x$ , known measurements  $y$ , parameters  $\theta$  and potential faults  $f$ . To use this model for FDII purposes, there has to be analytic redundancy. This means that there are parts of the model or subsystems of the form

$$M^* = \{e^*, x^*, y^*, \theta^*, f^*\} \quad (2)$$

such that the subsystem  $M^*$  contains more equations  $e^*$  than unknowns  $x^*$ .<sup>1</sup> This property is called analytic redundancy since there are more equations than needed to calculate the unknowns. If the degree of redundancy is exactly one, meaning that  $\text{card}(e^*) - \text{card}(x^*) = 1$ , the subsystem is called minimally over-determined and a single test can be formulated. The test used here uses input-output models which utilize the set or system of equations  $\{e^* \setminus e_i\}$  to calculate all  $x^*$  and the remaining equation  $e_i$  is used to test the system for consistency. The simplest way of doing this is by subtracting the left (LHS) from the right-hand side (RHS) of  $e_i$  and forming a residual

$$r(y^*, \theta^*, x^*) = \text{RHS}(e_i(x^*, y^*, \theta^*)) - \text{LHS}(e_i(x^*, y^*, \theta^*)). \quad (3)$$

For the sake of simplicity, the term residual will also include the calculation of  $x^*$  for the rest of the paper. If the measurements  $y^*$  are consistent with the model, the residual returns zero, since the left and right-hand side are equal. If the measurements aren't consistent with the model, the residual returns a value different from zero. If a connection between faults  $f^*$  and equations  $e^*$  of the subsystem has been defined, a residual can be used to test the system for the faults affecting its equations. For the defined subsystem above, a residual value different from zero would be an indicator that one of the faults  $f^*$  might be present.

Ideally, the defined residuals are equal to zero in the fault-free

<sup>1</sup>The asterisk denotes that the given sets are subsets of the full model.

case and different from zero in the case of a fault. In reality, however, this is not the case. Due to modeling errors and uncertainty in the measurements as well as parameters, the residuals are in practice almost always different from zero. To solve this problem, we published a method in (Mardt & Thielecke, 2021) which allows for a physical based statistical evaluation of the residuals under uncertainty to facilitate robust fault detection. The method uses uncertainty estimations for the parameter and sensor uncertainty gained from a-priori knowledge as well as multiple sensor readings. These uncertainty distributions are used to sample a set of possible residual values using Monte Carlo simulation (MCS). Thus, rather than single values for  $r$ , samples of the set of possible values  $S_r$  are generated. The test for consistency then becomes

$$\begin{aligned} 0 \in S_r &\quad \text{if } y^* \text{ consistent with } M^* \\ 0 \notin S_r &\quad \text{otherwise} \end{aligned} . \quad (4)$$

Since  $S_r$  is not known explicitly, the samples are examined to determine whether 0 is part of the set. This is done using Highest Density Regions (HDR), a method which returns the set  $S_{r,\alpha}$  which contain the most probable  $100(1-\alpha)\%$  of values as interval boundaries (Hyndman, 1996). The proposed consistency test is

$$\begin{aligned} y^* \text{ consistent with } M^* &\quad \text{if } 0 \in S_{r,\alpha} \\ y^* \text{ inconsistent with } M^* &\quad \text{otherwise} \end{aligned} . \quad (5)$$

E.g. for  $\alpha = 0.05$  the fact  $0 \in S_{r,\alpha}$  means that the measurements are consistent with the most probable 95 % of all possible systems. This method ties a probability parameter to the decision which allows controlling the false alarm rate, since for this example 5 % of the possible systems would lead to a detection and thus an alarm even though they are not faulty. Since this is a Monte Carlo based method which uses HDR to interpret the results, it will be subsequently called MCS-HDR.

Combining the information about which residual is sensitive to which fault, a detection and an isolation of the considered system can be conducted in a robust way using the MCS-HDR method, given that there are enough residuals. Fault identification goes further in the sense that it computes a value or range for a considered fault  $f$  to base immediate or future actions on that information. In (Mardt & Thielecke, 2021) we proposed a method which relies on the evaluation of multiple copies of the same residual with explicit fault inputs to decide which one fits best. This requires explicit fault models rather than just the information that a fault affects an equation. This method of fault identification is computationally expensive since it requires multiple MCS and HDR evaluations for the same fault. A simpler method which wasn't discussed in previous publications is the direct calculation of the fault input  $f$  using MCS HDR. When the equation  $e_i$  in Equation 3 is the one affected by a fault and is analytically solvable for that fault rather than just solving for 0, the MCS HDR method can

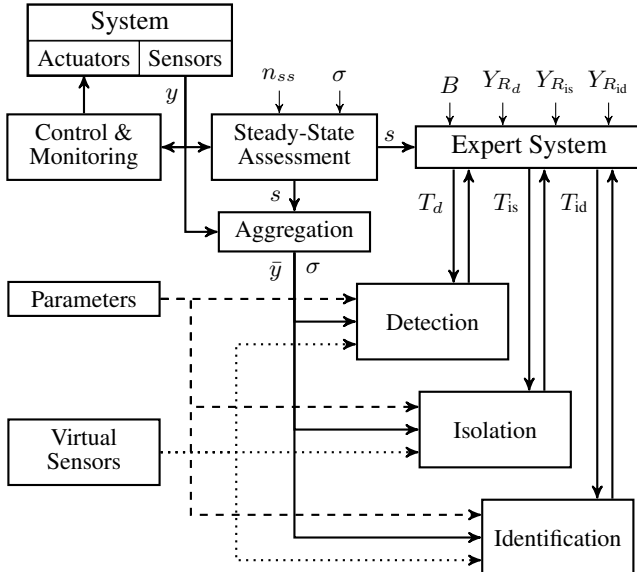


Figure 1. Proposed implementation architecture

be used to calculate the most probable intervals for the fault input directly. This new approach requires less computational power and leads to a better interpretability of the results compared to the comparison of multiple residuals with different fault inputs. Consequently, this method will be prioritized as long as the requirements are met.

## 2.2. Implementation of Model-Based FDII

To efficiently implement the abstract ideas of using non-linear models for FDII purposes, an actual architecture is needed. The proposed architecture is shown in Figure 1. The monitored system is shown in the top left. It consists of sensors and actuators which are connected through the control and monitoring of the system. The control and monitoring closes the control loop and ensures the safe operation of the system. All other shown blocks are part of the maintenance related FDII and will be discussed in the following paragraphs.

The first block which directly interacts with the system is the steady-state assessment block. It continuously monitors the sensor signals and determines whether a signal can be considered to be in steady-state. Since the residuals used for FDII are based on steady-state equations, they need steady-state sensor signals in order to provide valid results. The method used for steady-state detection is based on a sliding window standard deviation. Therefore, the standard deviation of each signal is constantly calculated over the last  $n_{ss,i}$  values and compared to a constant. This constant is based on the expected distribution of the sampling standard deviation of a normally distributed sensor signal with known standard deviation  $\sigma_i$  for  $n_{ss,i}$  samples. The output of the block is one binary signal  $s_i$  for each assessed measurement, which states if that signal is considered steady-state.

As soon as a signal is considered steady-state, the steady-state assessment block triggers the aggregation block. This block calculates the running mean  $\bar{y}_i$  and sample standard deviation  $\sigma_i$  of that signal as long as it is in steady-state and resets once it leaves steady-state. These two values per measurement are used as input to the MCS-HDR method used in the detection, isolation and identification blocks.

The expert system block is the supervising element for the FDII process. It continually receives the information about which measurements are in steady-state and holds the static information about which signals are used in which detection-residuals  $Y_{R_{d,j}}$ . Detection-residuals are a subset of all residuals which reliably detect all faults of the system. They are the first ones to be evaluated and set the starting point for the other diagnosis stages. When all signals were in steady-state and one of them switches state, the expert system triggers that specific detection-residual using the trigger signal

$$T_{d,j}(n) = \begin{cases} 1 & \text{if } \forall y_i \in Y_{R_{d,j}} : s_i(n-1) = 1 \text{ and} \\ & \exists y_i \in Y_{R_{d,j}} : s_i(n) = 0 \\ 0 & \text{else.} \end{cases} \quad (6)$$

The reason for that is, that this is the point in time when the most information about all the measurements has been gathered. An evaluation of the residual before that would lead to worse results.

The detection block uses the MCS HDR method explained in the previous chapter. It conducts an MCS to receive residual samples, which are then evaluated using HDR and a given  $\alpha_i$  for each residual. Whether 0 is part of the calculated HDR is fed back to the expert system by one boolean signal for each implemented residual. In addition to the measurements sample mean and standard deviation, the detection block also receive parameter samples from a database and samples from virtual sensors. Virtual sensors are variables of the system which aren't measured but can be estimated with some uncertainty. For example, the temperature of a fluid might be needed to calculate the density of said fluid. In practice, however, the benefit of actually measuring the temperature might be slim, and it could suffice to just assume that the temperature is somewhere in a plausible range. This is what virtual sensors do, they supply samples of sensors which aren't measured but estimated and allow including the uncertainty tied to that virtual measurement.

The expert system receives the results of the MCS-HDR evaluation of the detection-residuals and enables the isolation-residuals which are needed for the next diagnosis step. This is done based on the residual fault matrix  $B \in \mathbb{B}^{n_r \times n_f}$  where  $n_r$  and  $n_f$  are the number of total residuals and faults respectively. This matrix encodes the fact that a residual is sensitive to a specific fault. If the observed residual pattern from the detection-residuals suggests multiple possible single faults explaining that pattern, the respective isolation-

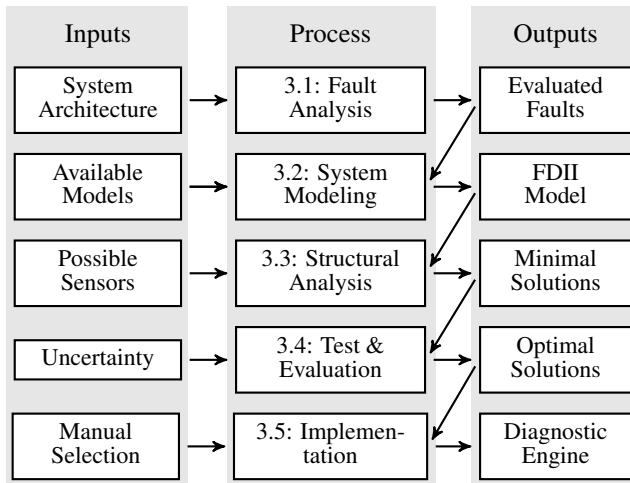


Figure 2. Design methodology

residuals are triggered. The isolation-residuals are another subset of all residuals and are needed to fully isolate all relevant faults from each other. The reason these aren't always evaluated is to save computation time, power and thus costs.

For the last step of the FDII the expert system enables the identification-residuals which correspond to the isolated faults to identify them and compute an actual health status. This is done by the identification methods discussed in the previous section. All residuals which fulfill the requirements for the direct computation of  $f$  are implemented accordingly. All other residuals use the indirect method presented in (Mardt & Thielecke, 2021).

### 3. A DESIGN METHODOLOGY FOR FAULT DIAGNOSIS SCHEMES

As explained in the previous section, the implementation uses certain measurements of the system to evaluate different sets of residuals for FDII purposes. The selection of these sensors and matching residuals is a difficult task, especially when the system under consideration is a complex one. To aid the system's designer in the process of choosing sensors and matching residuals during the design stage of the system, this section presents a design methodology. The general steps of this methodology are depicted in Figure 2 and chronologically examined in the following sections.

#### 3.1. Fault Analysis

The process of designing an FDII system, similar to almost all engineering processes, starts with the definition of requirements. In this case this is a list of component faults which shall be detected, isolated and identified. The general analysis proposed here is closely related to first steps of the MSG-3 aircraft industry standard for the planning of maintenance tasks (Air Transport Association, 2002).

The analysis starts by defining maintenance significant items (MSI). These are components from which a fault leads to: an interruption of service, a decrease of operational reliability, or comes with a significant economic impact. For these MSI, a failure mode and effect analysis (FMEA) is carried out. This means evaluating which failure modes a component may show and how they impact the rest of the system's operation. The third step takes these results and categorizes the MSI failure modes based on the impact (safety, operational, economic) and the type of manifestation for the operating crew (evident, hidden).

After assessing the effects of all faults and the baseline of onboard detection, the need for additional diagnostic steps by a dedicated FDII system can be evaluated. For the detection, this includes evaluating whether the detection of a hidden fault by a dedicated monitor is potentially less expensive than the operational costs induced by the same fault. This evaluation, like all economic considerations in this context, are not the focus of this work and thus not further discussed. There is a plethora of research on this topic for the interested reader. It's important to state that at this point the actual costs of isolating or detecting a fault are not yet evaluated and will be a result of step 4 of the methodology. Thus, the economic analysis has to use rough assumptions for the costs, which can be validated later in the process. If the costs are substantially different from the assumption, an iteration loop might be useful.

The formulation of isolation requirements should be straightforward and be based on maintenance routines. If two faults lead to the same maintenance action, i.e. replacement of a specific line-replaceable unit (LRU) there is no need to isolate them on-board. If on the other hand the two faults require different maintenance actions, the isolation is necessary to avoid unnecessary actions during the maintenance process. This trade-off could also be economically studied by actually calculating the cost of a maintenance iteration and the potential cost of the on-board isolation.

Similar to the steps above, the decision of whether a fault should be identified should be based on a cost benefit analysis. For components which degrade randomly or show complex degradation patterns while having a large operational impact, the identification or health monitoring becomes more valuable.

The final result of the fault analysis step is a table containing all MSI faults which shall be detected. For each fault, an isolation group is defined which states from which other faults it shall be isolated and a binary indication on whether the fault shall be diagnosed or not.

### 3.2. System Modeling

The second step of the proposed methodology is the system modeling. This step sets up the FDII model, which is subsequently analyzed in the following steps. As defined in Equation 1 a model consists of equations, variables, measurements, faults and parameters. Ideally, the equations of the physical behavior are already defined in available models from the system's design phase. In most cases, these available models only contain nominal behavior and the equations need to be extended with faulty behavior based on the fault inputs  $f$  if the requirements from the previous step include fault identification.

To simplify the modeling process and make the FDII models more maintainable, this method uses a custom JSON-based modeling environment. This object-oriented environment allows for the definition of general components which are stored in a library. These components can be instantiated and connected to build the actual system. By implementing an acausal modeling approach similar to Modelica or Simscape, the direction of physical ports is omitted and not of the users' concern. The connecting equations based on Kirchoff's laws are added automatically based on a defined topology of the system.

Since this step's goal is to set up the model for the structural analysis, only the structure of the model has to be defined. The actual parameters are not yet needed.

### 3.3. Structural Analysis

The third step of the presented design methodology is the structural analysis of the behavioral model created in the previous step. The goal of this step is to determine which possible minimal sensor combinations fulfill the FDII requirements specified during the fault analysis using the model created in the previous step.

The use of structural analysis to determine which faults are structurally detectable and isolable goes back to the work of (Cassar & Staroswiecki, 1997). They propose to analyze a bipartite graph  $G = (X, E, A)$  representing the structure of a system by mapping the variables  $X$  to the equations  $E$  they appear in by the edges  $A$ . Applying the Dulmage-Mendelsohn decomposition (DM) to  $G$  assigns each of the nodes in  $X$  and  $E$  to one of the three groups: under-determined, just-determined and over-determined. Equations in the over-determined part of  $E$  are considered monitorable. This means that they can be tested for consistency because there are more equations than variables in this part of the system, hence the name over-determined. Thus, it is structurally possible to build residuals out of these equations. The adjective structurally is important in this context because the structural analysis as it is defined for now does not take into account the actual equations of the system. Thus, solving

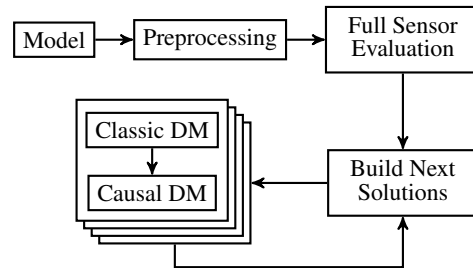


Figure 3. Sensor placement flow chart

over-determined subsystems may require numerical solvers or, in the dynamic case, integration.

The work of (Rosich, Frisk, Aslund, Sarrate, & Nejjari, 2011) takes the causal solvability of equations into account and presents a method to compute a DM which ensures causal solvability. This means the variables in the just and over-determined parts are explicitly calculable without the use of numerical solvers. To take the solvability into account, additionally to the equation itself, the information about for which variable the equation is solvable needs to be given.

The publication (Rosich et al., 2011) also adapts the sensor placement via structural analysis presented in (Krysander & Frisk, 2008) to only produce causal solvable results. Since the causal solvability poses additional restrictions on the sensor placement problem, the presented solution is a greedy brute-force search where costs of sensor sets are considered when choosing the next set to test. Thus, the placement can stop after a set has been found which fulfills the requirements, since it is the cheapest one to do so.

The sensor placement proposed here uses most of the concepts from (Rosich et al., 2011) to produce causal solvable solutions. For that reason, the library approach presented in Section 3.2 includes the information about which equations are solvable for which variables. Since the aim of this work is to also evaluate the robustness of sensor sets and thus tackle a multicriteria optimization, the causal sensor placement cannot be used as is and needs to be adapted. Due to limited space, a high level overview of the process is depicted in Figure 3 and will be discussed briefly in the following paragraphs.

To prepare the system of equations for the structural analysis, the first step of the sensor placement process is the preprocessing. This includes the elimination of redundant variables as well as mandatory transformations of the system of equations to ensure proper results. The elimination of redundant variables not only clarifies the equations and saves memory, it also reduces the number of sensor combinations needed to be evaluated by exploring equality between these sensors. If two sensors are structurally equal, only one of these sensors needs to be tested and the number of possible solutions is essentially halved. The transformation of the system of equa-

tion might be mandatory, since the structural analysis only assesses the structure of the system of equations. Consequently, the results depend on the formulation of the equations and can be altered through analytical transformation of the equation. Consider for example the two equations

$$\begin{aligned}x_1 &= x_2 + x_3 \\x_4 &= x_2 + x_3.\end{aligned}\quad (7)$$

This system of equation contains four unknown variables and two equations, and thus structural analysis comes to the conclusion that measuring two of these variables leads to the calculation of the other two. This holds for most cases but does not when measuring  $x_1$  and  $x_4$  since they're equal. To find these conflicts, which often occur in flow networks, algorithms are implemented to solve the equations and transform them into structurally unique representations like

$$\begin{aligned}x_1 &= x_2 + x_3 \\x_1 &= x_4.\end{aligned}\quad (8)$$

To assess whether the FDII requirements can be met with the available sensors and if all sensors are actually needed, the next step evaluates the full sensor model. This step is adapted from (Rosich et al., 2011) and modifies the requirements and list of possible sensors which are used in the next step.

After the preprocessing and evaluation of the model containing all sensors, the next step is the actual sensor placement. Since the goal is to find all minimal causal solvable solutions, all sensor combinations have to be evaluated, which leads to an exponentially complex problem. To account for this, the implemented algorithms are optimized for efficiency. This begins with the chosen search strategy. A breadth-first search is used, which analyzes all sensor sets of a given length first before evaluating the next length. This allows for the parallelization of the actual evaluation of the combinations, since the results of each evaluation do not affect the ones on the same level. Evaluating multiple solutions in parallel is one key element of making the evaluation of hundreds of thousands combinations possible. The other key element is the implemented evaluation strategy. Instead of evaluating the causal DM of the currently evaluated structure directly, a two-step method is applied. This tests the classic DM without the causality restrictions first and only if that fulfills the requirements, the much more computationally expensive causal DM analysis is conducted. Since a large amount of tested solutions does not fulfill the requirements, this approach immensely increases the efficiency. If a valid solution is found, this solution will not be expanded in the next step, since it is by definition a minimal one. The generation and evaluation of new solutions is repeated until no new solutions are possible.

### 3.4. Evaluation

After calculating all possible sets of sensors, they can be evaluated to choose an optimal one for the task at hand. The first and most straight forward is the evaluation of costs. This step sums the costs of each sensor in each combination and returns a single value for each set. The cost of each sensor is considered an input to this method and depends not only on the initial cost of the sensor itself and its installation, but also on the running cost of evaluating and maintaining that sensor.

The next evaluation step is the evaluation of the FDII performance of each sensor set. For each of the detection, isolation and identification steps, measures can be defined to assess the performance. For the detection, these are the rates of a false detection, namely the false alarm rate (FAR) and the missed detection rate (MDR). As explained in Section 2.1 the FAR considering a random system inside the defined bounds is defined by the  $\alpha$  value used in the HDR evaluation of the residuals. Consequently, this rate is an input parameter rather than something to evaluate. The MDR on the other hand is not known until evaluated in some form. To test the MDR, some faulty data is needed to use as input into the implemented residuals and assess if they detect the fault. In the development process of the system real data is generally not available and even if a prototype has been built it rarely produces the faulty data needed to test the residuals. The easiest way to get faulty data is the available model from the design process, which has been used to derive the diagnosis model. It's also possible to get data from the diagnosis model, but since it wasn't built for simulation and is not necessarily entirely solvable, this is a more tedious task.

To generate the faulty data, faults have to be injected into the system. It is assumed that all faults are easier to detect the higher their fault input  $f_i$  is. Thus, to evaluate the performance a minimum detection requirement for each fault has to be specified which is the fault value at which the data is created and the MDR evaluated.

Given that faulty data of the system is available, the residuals can be implemented and tested. To implement residuals, the over-determined part of the system including the set of sensors needs to be examined. This is done by calculating causally minimal structurally overdetermined sets of equations (MSO). These are the minimally overdetermined subsystems discussed in Section 2.1. There are usually plethora of MSO for each solution, and they all detect a subset of faults and can be implemented as a residual. To evaluate the MDR for a fault, all possible residuals that detect this fault have to be tested. The lowest MDR of all residuals for each fault is the best possible MDR for that solution. Note that it is assumed here that the number of implemented residuals is of no concern, and thus the best MDR can be achieved even if one residual for each fault has to be used. The detection evaluation results in the best achievable MDR for each fault for

each solution.

Note that the MDR depends on the chosen FAR, in a way that a higher FAR will lead to a lower or equal MDR. The correlation between the two depends on the width of the uncertainties. If the fault leads to a behavior which is entirely separated from the nominal behavior, both an FAR of 0 and an MDR of 0 are possible. If the faulty and nominal behavior overlap, this is not possible and a trade-off between the two has to be chosen.

To assess the isolation performance, the same MDR data is used as for the detection performance. Rather than assessing the MDR of all residuals for one fault, the MDR of each isolation combination is considered. I.e. if  $f_1$  and  $f_2$  are supposed to be isolated all residuals which detect  $f_1$  but not  $f_2$  are considered and the lowest MDR is taken for this category. Thus, the isolation evaluation results in one best achievable MDR for each required isolation combination for each possible solution.

The evaluation of the identification performance can also be conducted by applying the residuals to faulty test data. In this case, there are two evaluation criteria: the rate of correct classification and the accuracy in terms of an average width of the predicted health interval. The second criterion is only reasonable for the direct implementation of the fault identification, where an actual interval is calculated. For the indirect implementation, which assesses multiple fault intervals for the same residual, the width of the tested intervals is an implementation parameter.

### 3.5. Implementation

The Implementation is the last step of the proposed design methodology. It takes the chosen solution(s) and defined parameters and automatically generates the FDII engine seen in Figure 1. The engine is implemented into a Simulink model which can be connected to the design model for further testing or used for code generation to apply to a test rig for online execution.

## 4. APPLICATION

The following section describes the results of the application of the previously presented design methodology to a hydraulic power package (HPP). The section begins by introducing the HPP with all its components, purposes and operation modes. The following parts are structured according to the methodology, beginning with the fault analysis which leads to the modeling of the HPP followed by the structural analysis. The results from the analysis are subsequently analyzed and promising solutions are chosen for the final part of this section, the implementation and application to data from the actual HPP test rig.

### 4.1. System description

The HPP is a compact unit integrating two redundant pumps and the necessary hydraulic system equipment (reservoir, filters, valves). Due to the compact and modular design, it can be integrated into modern, More Electric Aircraft architectures to supply local hydraulic circuits. The modular approach enables operational benefits for installation, maintenance and testing. (Trochelmann, Rave, Thielecke, & Metzler, 2017)

The system architecture of the HPP is depicted in Figure 4. The two redundant motors, powered and controlled via an external power electronic unit, supply mechanical power to their connected pumps. The pump turns the mechanical into hydraulic power and pushes hydraulic fluid through a check-valve, which prevents flow reversal during one pump operation. After the check valves, the flows of the two pumps combine into a single one which flows through another check valve and the high pressure filter. After the high pressure filter, the fluid flows to the consumers via the high pressure port (HP). In case of a malfunction, the fluid can bypass the consumers through the pressure relief valve (PRV). The return flow arrives at the low pressure port (LP) and flows through the low pressure filter before entering the reservoir. From the reservoir, the fluid is sucked through a flow restriction. Every one of the components shown in Figure 4 is connected to the others via pipes not shown in the schematic.

For clarity, only measurement points in contrast to the actual sensors are depicted in Figure 4. The measured quantities for each of the points are listed in Table 1, where  $T$  is the temperature,  $p$  is the pressure,  $dp$  is the differential pressure,  $u$  is the voltage,  $i$  is the current,  $\omega$  is the angular velocity and  $V$  is the volumetric flow rate. The shown sensors are the ones installed on the test rig at the Hamburg University of Technology. Most of these sensors are installed for testing purposes and not necessarily needed for the operation of the HPP. The minimum set of sensors needed for a nominal operation depends on the chosen control and operating strategy. One possible set taken from (Trochelmann & Thielecke, 2021) is subsequently used and includes the following sensors  $\{T_{s2}, p_{s2}, u_{s7,8}, i_{s7,8}, \omega_{s9,10}, p_{s11,12}\}$ .

The HPP comprises redundant motor pumps for reliability purposes. This means that the HPP is sized to supply the connected hydraulic system with only one operable pump. Thus, in almost all modes of operation, only one pump is actively driving the connected system while the other one is on standby. Only in some, not safety-critical modes, both pumps are used to increase the delivered flow of the HPP. Consequently, only one pump operation is considered in the following analysis, since it massively reduces the system complexity and thus sensors and algorithms needed for the FDII of the HPP.

Note that the HPP test rig was not built to design or test FDII

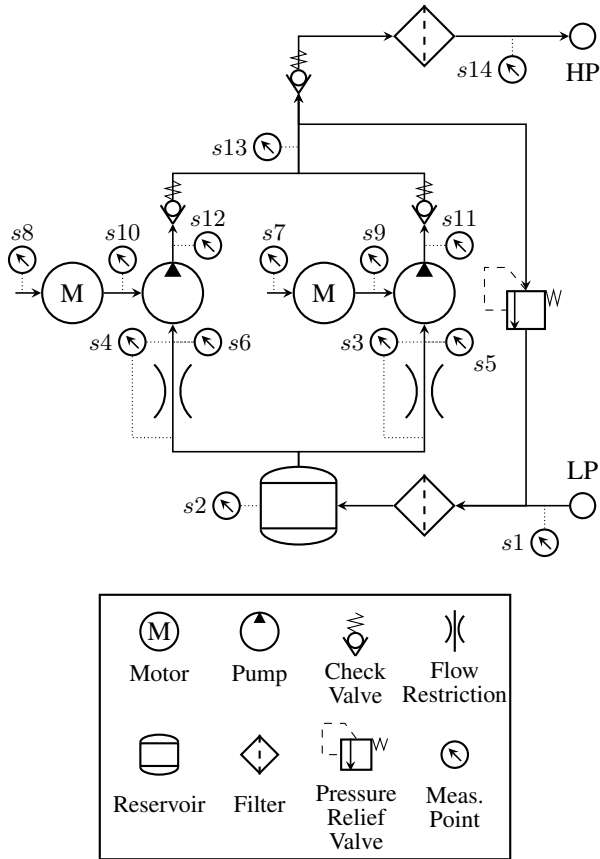


Figure 4. Hydraulic power package system schematic

methods and thus does not offer the possibilities to emulate faults of the system. The installed sensors were not chosen to diagnose the HPP, but rather to design control strategies and to validate models of the system.

#### 4.2. Fault Analysis

As described in Section 3 the first step of the presented method is the analysis of the faults of the system and the respective need for detection, isolation and identification. Basically, all the depicted components in Figure 4 are subject to degradation and need to be replaced at some point of the HPP life. It is important to keep in mind that a continuous observation of a component produces costs in the form of initial invest-

Table 1. Measurement points and quantities of the HPP

Sensors	Measured Quantities
$s_1, s_5, s_6$	$T$
$s_2, s_{14}$	$p, T$
$s_3, s_4$	$dp$
$s_7, s_8$	$u, i$
$s_9, s_{10}$	$\omega$
$s_{11}, s_{12}$	$p$
$s_{13}$	$\dot{V}, p, T$

Table 2. Results of the HPP fault analysis

Fault Name	Isol. Group	Identified
$f_{hm,pump}$	1	yes
$f_{vol,pump}$	2	yes
$f_{motor}$	3	yes
$f_{lp,filter}$	4	no
$f_{hp,filter}$	5	no

ments and running costs for the onboard sensors and computing power. Thus, for components which degrade on a large time frame, a continuous FDII produces more costs than it saves in maintenance. As explained above, the economic analysis of this is not part of the methodology of this paper. Consequently, the components and their FDII level have been selected according to engineering judgment.

The faults considered relevant for FDII purposes are listed in Table 2. The first one is the hydro-mechanical degradation of the pump  $f_{hm,pump}$ . This fault affects the ability of the pump to turn mechanical power on the shaft to differential pressure across the pump. It describes the torque loss due to friction on the mechanical and hydraulic side, hence the name. The second relevant fault is the volumetric degradation of the pump named  $f_{vol,pump}$ . This fault decreases the ratio between theoretical flow of the pump given by its speed and the actual hydraulic flow in the system. It is a measure for the amount of internal leakage in the pump. The third fault is a motor fault named  $f_{motor}$ . It is a lumped fault which affects the efficiency of the motor to turn electrical into mechanical power delivered to the pump. It combines mechanical friction as well as electrical losses in the motor. The fourth and fifth fault  $f_{lp,filter}$  and  $f_{hp,filter}$  represent the clogging of the filter on the low and high pressure side respectively. All of these faults shall be detected and isolated from each other. The reason for the isolation definition is to separate different faulty LRU to facilitate maintenance. The identification is limited to the motor and pump, since the degradation of these components is much more complex than the filter degradation and might benefit from a continuous health monitoring.

#### 4.3. System Modeling

As described in Section 3.2, ideally, there is already a model of the system under consideration present when starting the process of FDII design. This is the case for the HPP as well. Two models, one for the controller design and one for the thermal analysis of the HPP, are available. Both of these models model nominal dynamic behavior of the HPP and have been validated for their specific purpose using the real test rig. Having an already validated model is an ideal starting point to build an FDII system for that specific unit, but does only provide a small benefit when it comes to a general FDII scheme for all units of that kind.

Since both available models were built for different purposes,

their modeling scope is different. Therefore, the most accurate part of both models is combined to build a single steady-state model for FDII design. The resulting model uses the library concept described in Section 3.2 to model three different domains: an electrical one to represent the electrical interface of the HPP, a mechanical one to model the connection between the motor and the pump, as well as a hydraulic domain with temperature dependent fluid parameters to model the rest of the system. For most of the components, the equations used in one (or both) of the two existing models were used. For other components, which were out of scope in both of the models (i.e. the filters), manufacturer's information was used to build new models. The flow restriction is the only component which uses a polynomial fitted to test rig data to model the pressure loss, since it does not behave like a standard hydraulic component, i.e. an orifice.

None of the available models depicts faulty behavior of the components, which is why this had to be added to the equations. In contrast to the physical modeling of the components, the fault modeling approach is a more practical one. The hydro-mechanical pump and motor faults use an efficiency based approach

$$P_{\text{out}} = (\eta_{\text{nom}} - f) P_{\text{in}} \quad (9)$$

where  $P_{\text{in}}$  and  $P_{\text{out}}$  are the in and output power respectively,  $\eta_{\text{nom}}$  is the nominal efficiency and  $f$  is the fault input affecting the behavior. Thus, identifying  $f$  is directly related to the efficiency, an easily interpretable quantity. A similar approach is used for the volumetric degradation of the pump

$$\dot{V}_{\text{act}} = (\eta_{\text{nom}} - f_{\text{vol,pump}}) \dot{V}_{\text{th}} \quad (10)$$

with a nominal volumetric efficiency  $\eta_{\text{nom}}$  and the actual and theoretical flow  $\dot{V}_{\text{act}}$  and  $\dot{V}_{\text{th}}$  respectively.

#### 4.4. Structural Analysis

To analyze the structure of the model of the HPP and find applicable sets of sensors to fulfill the FDII requirements, the possible sensors have to be defined. The aim of this work is to test the resulting sensors sets on the real test rig. This comes with the restriction, that only sensors can be used which are available on the real test rig. Therefore, the list of possible sensors is the list of sensors installed on the real test rig listed in Table 1. To compute the sets of possible sensors, the approach presented in Section 3.3 is used, and the results are discussed in the following section.

The first step of the sensor placement process is the preprocessing. During this process, the model is simplified and redundant variables and sensors are discovered. For the HPP, this step reveals that the sensors  $T_{s13}$  and  $T_{s14}$  measure the same quantity. This comes from the fact that no heat loss is modeled in the piping, hp filter and check valve between  $s_{13}$  and  $s_{14}$ . This means only one of these sensors has to be con-

sidered during the sensor placement, and the results can be expanded for the other sensor.

The evaluation of the model containing all sensors is the second step of the sensor placement and shows that a degradation of the filter on the low pressure side of the HPP is not possible. This is due to the fact that there is no pressure sensor upstream of the filter, which does not allow calculating the differential pressure by any means. Thus, the actual differential pressure cannot be compared to the theoretical and consequently this fault cannot be detected. All other faults are structurally detectable. The isolability analysis shows that even with all possible sensors in place, a degradation of the motor  $f_{\text{motor}}$  cannot be isolated from a hydro-mechanical fault of the pump  $f_{\text{hm,pump}}$ . The reason for that is that both faults act on the power conversion from electric to mechanical and then hydraulic. Since there is no full measurement of the mechanical power in between the units, the faults cannot be separated. It would need an additional torque sensor at  $s_{9,10}$  to differentiate between the faults. This fact is acceptable since the motor and pump are part of the same LRU, so replacing one inevitably means replacing the other as well. This also implies, that a fault identification of both faults is not possible. One solution for this would be to combine both faults into a single one on the modeling side.

The full sensor analysis also identifies sensors which are not needed for the achievable FDII requirement. Since  $f_{\text{lp,filter}}$  is not detectable, the sensor  $T_{s1}$  is not needed to fulfill the updated FDII requirements and will be removed for the sensor placement. The reason this sensor is not identical to  $T_{s2}$  is that the fluid temperature in the reservoir is considered different from the one in the return line, which makes  $T_{s1}$  obsolete.

The structural sensor placement returns 30 possible sets of sensors, which are listed in Table 3. The actual number of possible sets has to be increased to 54 since 24 of the 30 solutions contain the sensor  $T_{s13}$  which can be replaced with  $T_{s14}$  as explained above. The following analysis omits the additional 24 solutions since they are structurally and in terms of uncertainty identical to their counterparts. Due to the limited space available here, an explicit in-depth verification of all possible sensor sets will not be provided. Instead, the following paragraphs will discuss why some sensor combinations are present in the solution sets.

To detect a volumetric pump fault, the theoretical and actual flow rate need to be compared to test the Equation 10 for consistency. The theoretical flow rate  $\dot{V}_{\text{th}}$  can be computed using the pump's displacement and the angular velocity measuring  $\omega_{s9}$ . If the angular velocity is not directly measured, it can be computed using the motor equations and measuring the voltage  $u_{s7}$  and current  $i_{s7}$ . The actual flow rate can be measured directly by using  $\dot{V}_{s13}$ . An alternative way is to compute it using the measurements  $dp_{s3}$  and  $T_{s5}$  as well as the flow restriction equations to get the flow rate. This low pressure flow

Table 3. Sensor overview

<i>s</i>	1	2	3	4	5	6	7	8	9	10	11	12	13	14	15	16	17	18	19	20	21	22	23	24	25	26	27	28	29	30
$T_{s2}$	1	1	1	1	1	1	1	1	1	1	1	1	1	1	1	1	1	0	0	0	1	1	1	1	1	1	0	0	0	
$T_{s5}$	1	1	1	1	1	1	1	1	1	1	1	1	0	0	0	1	1	1	1	1	0	0	1	1	1	0	1	1	1	
$T_{s13}$	1	1	1	1	1	1	1	1	1	1	1	1	1	1	0	0	0	1	1	1	1	1	0	0	1	0	1	1	1	
$V_{s13}$	0	0	0	0	0	0	1	1	1	1	1	1	1	1	1	1	1	1	1	1	1	1	1	1	1	1	1	1	1	
$dp_{s3}$	1	1	1	1	1	1	0	0	0	0	0	0	0	1	1	1	1	1	1	1	1	1	1	1	1	1	1	1	1	
$i_{s7}$	0	1	1	0	1	1	0	1	0	1	0	1	0	1	1	0	1	1	0	1	1	0	1	1	1	0	1	1	1	
$\omega_{s9}$	1	0	1	1	0	1	1	0	1	1	0	1	1	0	1	1	0	1	1	0	1	0	1	1	1	0	1	0	1	
$p_{s11}$	1	1	1	0	0	0	1	1	1	0	0	0	1	1	1	1	1	1	1	1	0	0	0	0	0	0	0	0	0	
$p_{s13}$	0	0	0	1	1	1	0	0	0	1	1	1	0	0	0	0	0	0	0	0	1	1	1	1	1	1	1	1	1	
$p_{s2}$	1	1	1	1	1	1	1	1	1	1	1	1	1	1	1	1	1	1	1	1	1	1	1	1	1	1	1	1	1	
$p_{s14}$	1	1	1	1	1	1	1	1	1	1	1	1	1	1	1	1	1	1	1	1	1	1	1	1	1	1	1	1	1	
$u_{s7}$	1	1	0	1	1	0	1	1	0	1	1	0	1	1	0	1	1	0	1	1	1	0	1	1	0	0	1	1	0	

rate needs to be converted to the pump's high pressure flow rate by calculating the mass flow through the system by measuring the reservoir temperature  $T_{s2}$  and turning that into the high pressure flow rate by measuring the high pressure temperature  $T_{s13}$ . Another option is to measure the flow's impact instead of calculating or measuring it explicitly. Thus, by measuring two of the high pressure sensors  $p_{s11,13,14}$  the theoretical pressure difference between them due to the theoretical flow can be compared to the actual pressure difference measured. Thus, the sensor sets needed for the detection of the volumetric pump fault are the ones fulfilling the expression

$$(\omega_{s9} \vee u_{s7} \wedge i_{s7}) \wedge (\dot{V}_{s13} \vee dp_{s3} \wedge T_{s5} \wedge T_{s2} \wedge T_{s13} \vee (p_{s11} \wedge p_{s13} \vee p_{s11} \wedge p_{s14} \vee p_{s13} \wedge p_{s14})). \quad (11)$$

In fact, all listed solutions are valid with respect to this expression. Similar expressions can be set up for the detection and isolation of the other components. This considerably small example shows that this is a tedious and error-prone task to do manually, which is why the structural analysis is a valuable tool.

#### 4.5. Evaluation

The first step of the evaluation is to assess the costs of all sensor combinations. Therefore, costs for each sensor have to be defined. For the sake of simplicity, only the procurement costs are taken into account and costs for maintaining the sensors are neglected. The costs for sensors which are considered already installed in the system are set to 0. The normalized resulting costs of all sensor sets can be seen on the sensor axis of Figure 5. These costs are widely spread, ranging from 0.36 (solution 1) to the maximum cost (solutions 28,29 and 30).

To choose a sensor set, the presented methodology not only uses the costs of the sensor sets, but also their robustness. For the detection problem, this is measured using the minimum achievable MDR of each sensor set. To test the sensor sets, a steady-state model of the whole system is used to generate

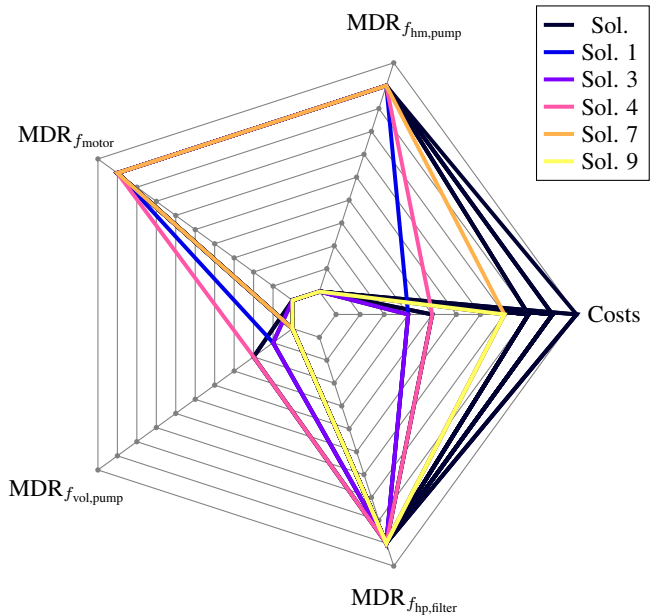


Figure 5. MDR and normalized costs of all 30 solutions with axis ranging from zero to one from the inside out.

faulty test data. The parameter and sensor uncertainties of the test model are the same as the model uncertainties and the minimum detection requirement is set to 0.2 for all faults but the volumetric pump fault, which is set to 0.3. The resulting MDR are shown on their specific axes in Figure 5. Solutions that will be discussed in the following are colored.

It is apparent that all the solutions have a high MDR for the high pressure filter faults. This is due to the relatively low accuracy of the pressure sensors  $p_{s11}$ ,  $p_{s13}$  and  $p_{s14}$  combined with the uncertainties of the other flow restrictions (check-valves and pipes) in between the sensors. The deviation in pressure drop due to the required minimal detectable fault is lower than the combined uncertainty of the sensors and parameters, and thus the defined detection specification cannot be met. For this reason, most applications of filter clogging detection use differential pressure sensors, which are much

more accurate than the difference of two absolute pressure sensors. This option wasn't considered here, since such a sensor is not installed on the test rig.

Particularly high MDR rates can also be observed for some solutions for the hydro-mechanical pump and motor faults. A comparison of the sensors used by these solutions shows that all the poorly performing solutions use a combination of  $u_{s7}$  and  $\omega_{s9}$  to calculate the theoretical differential pressure of the pump to compare it with the actual differential pressure applied to the system. Since the torque of a motor and thus the differential pressure of the connected pump is mainly driven by the current through the motor, measuring  $i_{s7}$  directly results in less uncertainty than calculating  $i_{s7}$  from  $u_{s7}$  and  $\omega_{s9}$ . In fact, the uncertainties in the parameters involved in the calculation are too high to make these solutions feasible. An analysis of these parameters shows that the magnetic flux linkage parameter of the motors is the reason for these uncertainties. This parameter is modelled as a uniform distribution spreading 10 % around the most probable value. Decreasing this uncertainty alone can turn the originally unfeasible into a feasible one.

The achievable MDR for the volumetric pump faults range from around 0 to 20 % forming one cluster each at 0, 10 and 20 %. The cluster at 0 % contains all sensor sets which measure the volumetric flow  $\dot{V}_{s13}$  directly. This introduces less uncertainty into the detection than calculating this flow from differential pressure measurements or measuring the effect of the flow on the high pressure side, and thus shows the least MDR. The second cluster around 10 % contains the solutions which measure the effect of the actual flow in the system by using the pressure differential of the sensors  $p_{s11}$  and  $p_{s14}$  (solutions 1,2,3). These solutions perform better than the ones using  $p_{s13}$  and  $p_{s14}$  due to the fact that more components between the sensors lead to a higher overall pressure drop and thus a more accurate detection. The sensor sets using  $p_{s13}$  and  $p_{s14}$  (solutions 4,5,6) form the cluster around 20 % and show the worst performance. Both, the residuals using the measured pressure differential on the high pressure side and the ones using the differential pressure  $dP_{s3}$  to compute the actual flow show a similar performance.

Due to the high relative price of a volumetric flow sensor, the best performing solutions for the volumetric flow fault are also the most expensive ones. Thus, it might be beneficial to further analyze the other solutions when lowering the requirements. This is done for three of the solutions (1,4,7) - each from one of the discussed clusters - in the next paragraphs.

The MDR calculated above depend on the minimum detection requirements defined for each fault. To assess how the MDR changes and if some solutions with higher MDR become feasible when the detection requirement is lowered, an analysis is carried out. The results of this analysis are shown in Figure 6. It shows the expected behavior that when the

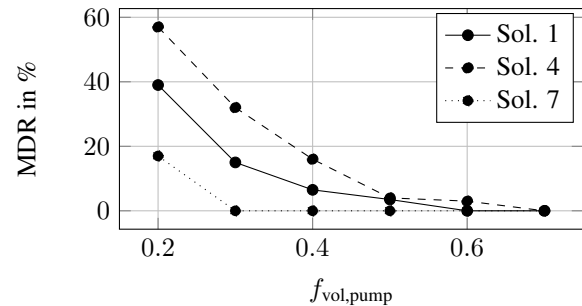


Figure 6. Missed detection rates for the volumetric pump fault for the solutions 1, 4 and 7 based on the minimum detection requirement for a  $\alpha = 0.05$

requirement is increased, the MDR decreases for each of the solutions. It can be seen that lowering the requirement would increase the MDR of solution 7 to an infeasible value. Increasing the requirement on the other hand leads to substantial lower MDR for the other solutions, which could make them feasible if the higher detection requirement is acceptable. This shows that the minimum detection requirement has a severe impact on the MDR and has to be assessed carefully when choosing or dismissing solutions.

As stated in Section 3.4, the MDR depend on the selected  $\alpha$  for the HDR calculation. For the rates shown above the selected  $\alpha$  is 0.05 resulting in an FAR of 5 %. Analyzing the effect of  $\alpha$  on the resulting MDR of a solution can help to optimize the solutions and assess their potential. Figure 7 shows the impact of the FAR on the MDR. The general expected behavior - a decrease in the MDR with increasing FAR - can be observed. This analysis also shows, that even with a substantially increased FAR, the solutions 1 and 4 still show an infeasible MDR. The MDR of solution 7 does not increase when lowering the FAR below the initial 5 %. This suggests that the minimal faulty behavior does not overlap with the nominal behavior at all, and a strict separation of both states is possible. This shows the importance of the analysis of the FAR on the MDR since the solution 7 can achieve better results with a lower FAR.

The evaluation of the isolation is not shown here due to space limitations. To assess the identification performance of the solutions, the two best performing ones with the lowest costs are compared. These are the solutions 3 and 9 as they perform well both for the detection of motor and hydro-mechanical faults as well as for the volumetric pump faults while having the lowest costs in their specific cluster.

To evaluate the identification performance of the chosen solutions they have to be implemented for identification either in the direct or indirect form. As stated in Section 3.4 this evaluation is based on two measures: the rate of correct classification and the average spread of the predicted health inter-

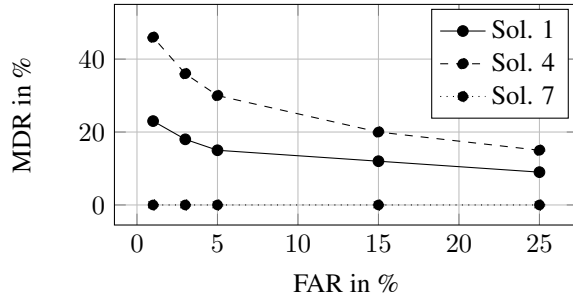


Figure 7. Missed detection rates for the volumetric pump fault for the solutions 1, 4 and 7 based on the FAR used for HDR calculations with a fixed minimum detection requirement of 0.3

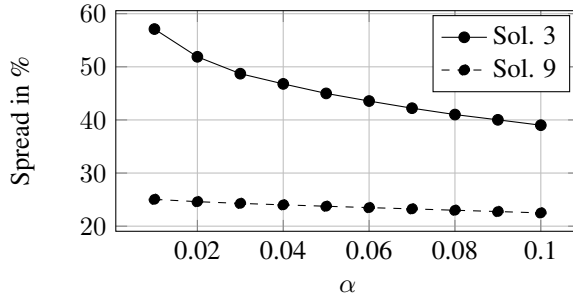


Figure 8. Spread of the identified health grade for the fault  $f_{vol,pump}$  for the solutions 3 and 9.

val. Since the spread of the predicted health is only assessable for the direct implementation and comparing directly and indirectly implemented results is a complicated task, only the best directly implementable residuals are compared here.

The results of the identification analysis are depicted in Figure 8. The figure shows the spread over the chosen  $\alpha$  for the HDR calculation of the health interval. The rate of correct classification is not shown, since it's - similar to the FAR - directly related to  $\alpha$ . Sampling a random system in the specified uncertainty bounds will lead to a correct classification rate of  $100(1 - \alpha)\%$ . The spread shows a similar behavior as the MDR above. For the solution 9 which measures the flow directly, the results are much more accurate than for the solution 3. The only directly implementable residual for solution 3 uses the differential pressure over the flow restriction  $dp_{s3}$  to indirectly measure the flow. These residuals were part of the worst performing cluster in the MDR analysis of the volumetric pump fault, and thus the results observed here are similar. Even when  $\alpha$  is increased substantially, the spread of solution 3 is still worse than the best results of solution 9. This comes with the downside of a much higher cost for solution 9 compared to 3 due to the costly volumetric flow sensor.

#### 4.6. Implementation

The following section shows the application of the chosen solutions to real sensor data of the HPP test rig. As explained above, the test rig was not built to design and test FDII schemes, and thus it has no ways to emulate faults of the system. Consequently, the applied solutions 3 and 9 should not detect any faults. In fact, this is the observed behavior. In none of the tested cases, any of the detection residuals detected a fault. This proves that the chosen parameter uncertainty intervals cover the behavior of the HPP test rig, however, it does not prove that faults can be detected and show the modeled behavior. Even though the test rig does not show any faults, one of the conducted analysis is presented in the following section.

One of the tests is shown in Figure 9. The first two panels show the normalized sensor signals for the pump volumetric flow and the angular velocity of the pump respectively. The gray lines show the raw sensor data and the black lines the mean of that signal for the current steady-state identified by the steady-state assessment and aggregated by the aggregation blocks shown in Figure 1. The areas where no mean is shown are considered transient. These sensor signals are used in the fault identification residual of solution 9. It detects volumetric pump flows by comparing the theoretical flow deduced from the speed of the pump with the actual measured flow. The vertical dashed lines show points in time when an evaluation of this MSO would be conducted, given it is triggered by the expert system or implemented as a detection residual. Note that the high flow phase after 40 s is not long enough for the signals to reach steady-state, and thus no residual is triggered.

Since the applied diagnostic engine doesn't detect any faults, the implemented identification residuals are not triggered automatically. To still be able to show results of the fault identification, these residuals are triggered manually to produce the results shown in the last panel of Figure 9. The dark grey bars show the range of the most probable 95 % of fault values for the volumetric pump fault  $f_{vol,pump}$  identified by solution 9. Each bar's height marks the identified range and is spread over the entire steady state length. It is apparent that the bars are shallower than predicted in Section 3.4. This is due to the fact, that only the plausible values in  $[0, 1]$  are shown. The actual identified interval also include values below 0. This increases the accuracy for the identification of faults near 0. For the analysis around 25 s this effect leads to a particularly shallow interval of  $[0, 0.09]$ . In fact, for all the shown analysis, the identified interval is smaller for points with higher flow through the system. This comes from the increased volumetric efficiency of pumps for higher flows. The underlying model doesn't model this dependency and uses a nominal efficiency coefficient as shown in Equation 9. To cover all modes of operations with low and high flows, this effi-

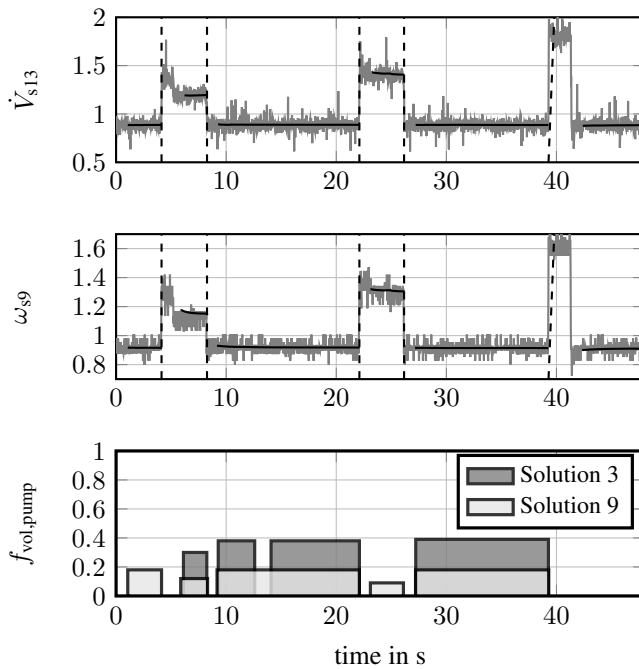


Figure 9. Raw and processed test rig sensor data as well as the identified fault intervals

iciency parameter has to have a rather wide uncertainty. Consequently, when the pump has a high volumetric efficiency in high flow operating modes, the potential fault cannot take on high values, since the parameter is already at its plausible end. This fact increases the accuracy for high flow operating modes and shows that the tested unit probably has a health grade of close to one. This suggests that modeling the flow rate dependent volumetric efficiency explicitly could improve the diagnosis results. For the FDII architecture itself, this suggests that aggregating the health status over multiple evaluation points could lead to overall better results.

The lower panel of Figure 9 also shows results for the evaluation of the identification residual of solution 3 in light gray. The steady state phases and thus points in time when the residual is evaluated differ from the ones for solution 3 since different sensors are used and the steady-state of these sensors is slightly different from the once used before. The general results show the predicted behavior during the evaluation of the results. Solution 3 performs worse than 8 due to the indirect flow measurement. The health grade intervals are generally twice as wide. The effect of narrower intervals for higher flows can be observed as well, but isn't as noticeable since the superimposed uncertainties from the added equations shadow that effect.

## 5. CONCLUSION

This paper presents a methodology to design robust model-based maintenance focused FDII schemes. The FDII engine itself utilizes the statistical evaluation of model-based residuals using Monte-Carlo simulations and highest density regions. This allows to consider measurement and parameter uncertainties when evaluating residuals, which increases the robustness of the method. The design methodology employs the structural analysis of available design models of the system to propose possible FDII schemes as minimal sensor sets. These sets are subsequently tested for their fault sensitivity to facilitate a sound selection of optimal solutions.

The application of the presented methodology to an aircraft hydraulic power package shows the advantages gained by applying a structured method in an FDII design process. The structural analysis of the behavioral model of the HPP reveals that even with all considered sensors in place, the low pressure filter fault is not detectable and the motor and the hydro-mechanic pump faults are not isolable from each other. Additionally, the structural analysis shows that there are 54 possible sensor sets which fulfill the FDII requirement. Calculating these solutions manually would be a tedious and error-prone task, which is significantly eased by the use of structural analysis.

The subsequent evaluation of all possible sensor sets in terms of costs and robustness reveal their differences in a quantifiable way. This step shows that the combined uncertainties in the measurements and parameters lead to a practically undetectable high pressure filter fault. This illustrates the importance of the evaluation of the results and that structural analysis can produce practically unfeasible solutions. In addition, the evaluation helps to assess trade-offs, as shown by the comparison of the accurate but also expensive direct measurement of the volumetric flow and its indirect counterpart.

The application of selected solutions to a real test rig proves that the modeled nominal behavior matches the real data and the selected solutions do not produce any false alarms. The identified health grades of the real test rig are also in line with the assumed nominal components. Since the test rig is not capable of emulating faults of the system, the diagnostic capabilities cannot be tested entirely. This does not reduce the scope of validation of the method, but rather of the used model's accuracy.

## ACKNOWLEDGMENT

This work was funded by the German Federal Ministry for Economic Affairs and Climate Action within projects RTAPHM (contract code: 20X1736M) and MODULAR (contract code: 20Y1910G) in the national LuFo program. Their support is greatly appreciated.

Supported by:



Federal Ministry  
for Economic Affairs  
and Climate Action

on the basis of a decision  
by the German Bundestag

## REFERENCES

- Air Transport Association. (2002). *ATA MSG-3 Operator/Manufacturer Scheduled Maintenance Development* (Tech. Rep. No. 2002.1). Air Transport Association.
- Cassar, J., & Staroswiecki, M. (1997). A structural approach for the design of failure detection and identification systems..
- Hyndman, R. J. (1996). Computing and graphing highest density regions. *The American Statistician*, 50(2), 120–126. (Publisher: Taylor & Francis Group)
- Krysander, M., & Frisk, E. (2008). Sensor placement for fault diagnosis. *IEEE Transactions on Systems, Man, and Cybernetics-Part A: Systems and Humans*, 38(6), 1398–1410. (Publisher: IEEE)
- Mardt, F., & Thielecke, F. (2021, June). Robust Model-Based Fault Detection Using Monte Carlo Methods and Highest Density Regions. In *6th European Conference of the Prognostics and Health Management Society PHM*. PHM Society.
- Rosich, A., Frisk, E., Aslund, J., Sarrate, R., & Nejjari, F. (2011). Fault diagnosis based on causal computations. *IEEE Transactions on Systems, Man, and Cybernetics-Part A: Systems and Humans*, 42(2), 371–381. (Publisher: IEEE)
- Trochelmann, N., Rave, T., Thielecke, F., & Metzler, D. (2017). An investigation of electro-hydraulic high efficient power package configurations for a more electric aircraft system architecture. In *Deutscher Luft- und Raumfahrtkongress DLRK*.
- Trochelmann, N., & Thielecke, F. (2021). Control Strategies for a Dual AC Motor Pump System in Aircraft Hydraulic Power Packages. In *The 17th Scandinavian International Conference on Fluid Power, SICFP'21, May 31- June 2, 2021, Linköping, Sweden*.